

Ionization Dynamics of Helium Dimers in Fast Collisions with He⁺⁺

J. Titze,¹ M. S. Schöffler,² H.-K. Kim,¹ F. Trinter,¹ M. Waitz,¹ J. Voigtsberger,¹ N. Neumann,¹ B. Ulrich,¹ K. Kreidi,³
R. Wallauer,¹ M. Odenweller,¹ T. Havermeier,¹ S. Schössler,¹ M. Meckel,¹ L. Foucar,⁴ T. Jahnke,¹ A. Czasch,¹
L. Ph. H. Schmidt,¹ O. Jagutzki,¹ R. E. Grisenti,¹ H. Schmidt-Böcking,¹ H. J. Lüdde,⁵ and R. Dörner^{1,*}

¹*Institut für Kernphysik, Goethe-Universität Frankfurt am Main, Max-von-Laue-Str.1, 60438 Frankfurt, Germany*

²*Lawrence Berkeley National Laboratory, 1 Cyclotron Road, Berkeley, California, 94720, USA*

³*GSI Helmholtzzentrum für Schwerionenforschung GmbH, Planckstr. 1, 64291 Darmstadt, Germany*

⁴*Max-Planck-Institut für Kernphysik, Saupfercheckweg 1, 69117 Heidelberg, Germany*

⁵*Institut für Theoretische Physik, Goethe-Universität Frankfurt am Main, Max-von-Laue-Str. 1, 60438 Frankfurt, Germany*

(Received 23 September 2010; published 20 January 2011)

By employing the cold target recoil ion momentum spectroscopy technique, we have investigated the (He⁺, He⁺) breakup of a helium dimer (He₂) caused by transfer ionization and double capture in collisions with alpha particles ($E = 150$ keV/u). Surprisingly, the results show a two-step process as well as a one-step process followed by electron exchange. In addition, interatomic Coulombic decay [L. S. Cederbaum, J. Zobeley, and F. Tarantelli, *Phys. Rev. Lett.* **79**, 4778 (1997).] is observed in an ion collision for the first time.

DOI: 10.1103/PhysRevLett.106.033201

PACS numbers: 34.50.-s, 34.70.+e, 36.40.-c

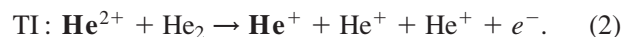
The existence of the helium dimer has been controversial for a long time. Starting from the first theoretical prediction by Slater in 1928 [1] a series of theoretical efforts (see e.g., [2–4]) and a few experimental studies [5,6] tried to resolve that controversy. In 1994, finally, Schöllkopf and Toennies [7] provided undisputed experimental evidence by diffracting a cooled helium gas jet from a transmission grating. In subsequent studies the average bond length and the binding energy were found to be 52 Å and 95 neV [8], respectively. These results highlight the unique character of the helium dimer as the largest, most delocalized and most weakly bound diatomic system.

In the present Letter we explore the interaction of this extreme quantum system with a fast ion. While ion-atom and ion-molecule collisions have been studied for decades in great detail the extreme nature of the helium dimer gives rise to a new reaction pathway unseen or unidentified in such collisions before. First our ion impact data show a strong channel of a process termed interatomic Coulombic decay (ICD). ICD was first predicted by Cederbaum and co-workers [9] for weakly bound compounds of matter. In this process, excitation energy is transferred via a virtual photon exchange from one atom to a neighboring atom where a low energetic electron is emitted. So far ICD has been only observed following photoionization [10,11]. As recently reported [12–14], this decay channel turned out to be an important source of low-energy electrons even in water. Thus, the demonstration of ICD induced by charged particle impact can be expected to be of relevance for radiation damage to living tissue by ions [15].

Second, we found a sequential two-center, two-electron process showing an extremely strong dependence on the molecular orientation. This observation in turn allows for a

novel type of test of the impact parameter dependence of the capture and ionization process. Since the days of Rutherford, the way to access the impact parameter in a collision is the measurement of the transverse momentum exchange between the projectile and the target nucleus. For ionizing and capture collisions in outer shells, however, the electron being emitted to the continuum or transferred to the projectile significantly contributes to the transverse momentum balance. This fact usually precludes Rutherford's approach to measuring the impact parameter. We will show that the measured distribution of the orientation of the helium dimer at the instant of the collision can be interpreted as a measurement of the impact parameter dependence of ionization and capture process which is inaccessible otherwise.

We have investigated collisions with 150 keV/u alpha particles in which both atoms of the dimer become ionized:



The projectile before and after the collision is shown in bold. In the first reaction, two electrons are captured to bound states of the projectile (double capture, DC), while in reaction (2) one electron is captured to a bound state and the second is emitted to the continuum (transfer ionization, TI). In either case, both centers of the dimer are charged and driven apart by their mutual Coulomb repulsion after the reaction. Using the cold target recoil ion momentum spectroscopy technique [16,17] we detected the charge state and momentum vectors of all particles. Thus, two singly charged ions emerging from a dimer breakup could be clearly distinguished from random events by checking

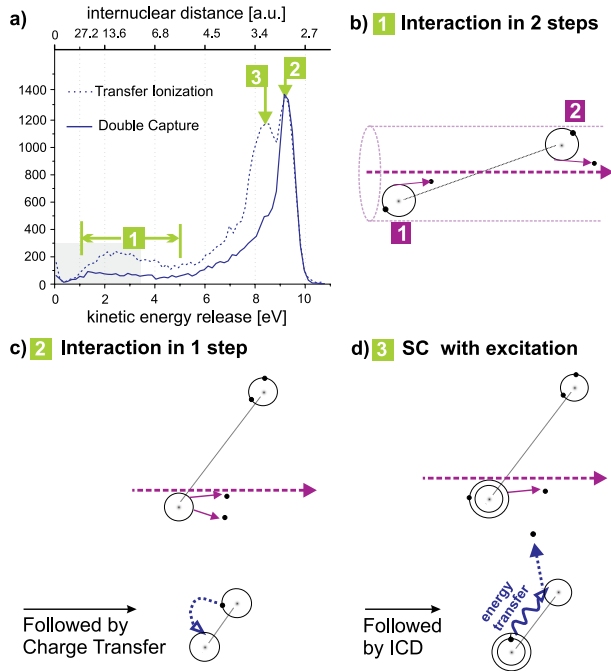


FIG. 1 (color online). (a) Distribution of the KER after breakup into He^+/He^+ for DC and TI [Eq. (1) and (2)]. The grey area indicates the region of decreased detection efficiency. Based on geometrical arguments, we have estimated that this reduces the measured cross section of the two-step process by a factor of 2. (b)–(d) Sketches of the sequence of events leading to the different peaks in (a); see text.

for momentum conservation and the back-to-back emission characteristic.

Our experiment was performed at the van de Graaff accelerator at the University of Frankfurt. The helium dimers were created in a precooled supersonic gas jet which was intersected by 90° with a beam of alpha particles (150 keV/u). By means of electric (12.9 V/cm) and magnetic (11.8 Gauss) fields, the ions and electrons produced in the interaction zone were guided towards two position and time sensitive detectors [18]. The momenta the ions gain in such an explosion are equal in magnitude, but oppositely directed. After being charge-state analyzed by an electrostatic deflector the projectiles reached a third position and time-sensitive detector. By measuring the time-of-flight and the position of impact, the three-dimensional momentum vector of each particle is obtained.

Figure 1(a) shows the kinetic energy release (KER) distribution, i.e., the energy of the ionic fragments in the target center-of-mass frame, for DC (solid line) and TI (dotted line). Surprisingly, the spectrum shows several maxima, even though the He_2 vibrational wave function is highly delocalized and structureless. The broad maximum between 1 eV and 5 eV and the very narrow peak at 9 eV which are seen for TI and DC suggest that the mechanisms leading to these particular values of KER must be similar for both reactions. For TI, the spectrum

exhibits an additional peak at 8 eV. This points towards a possible third pathway where a free electron seems to play a crucial role. In the following discussion we will identify the reaction pathways leading to these maxima in the KER distribution.

Within the reflection approximation the measured KER can be related to the internuclear distance R at the instant when finally both atoms are ionized

$$\text{KER (a.u.)} = \frac{1}{R}. \quad (3)$$

For the helium dimer, Eq. (3) has recently been shown to be a rather crude approximation due to the large extent of the He_2 wave function [19,20]. For our qualitative discussion below we nevertheless make use of this approximation. The R values obtained by Eq. (3) are shown as a second scale on top of Fig. 1(a). The different peaks in the KER hence indicate that processes leading to the final charging of the two dimer centers occur at different internuclear distances.

To further unravel the origin of the different peaks in the KER we now examine the angular distribution of the $(\text{He}^+, \text{He}^+)$ breakup direction with respect to the projectile beam axis. As it is shown in Figs. 2(a) and 2(b), the angular distribution leading to the low-energy maximum 1 is extremely narrowly peaked along the beam axis. Compared to studies on typical ion-molecule collisions (see e.g., [21–23]) this strong alignment is highly unusual and illustrates the existence of a two-step process where the projectile interacts independently with each of the two helium atoms. Such a sequential interaction can only occur when the projectile passes sufficiently close to both helium atoms. The impact parameter range contributing significantly to the capture or ionization signal is small compared to the internuclear distances leading to a KER of 1.0 eV up to 5.0 eV [$R = 5.5$ a.u.–29 a.u., according to Eq. (3)]. Therefore any two-step process selectively ionizes only those dimers which are aligned parallel to the beam [see sketch in Fig. 1(b)]. As the FWHM in Figs. 2(a) and 2(b) shows, the angular distribution is narrower for DC than it is for TI. This difference in the maximum tilt angles for TI and DC is a direct consequence of the impact parameter dependence of these processes. At the projectile velocity investigated here, electron capture requires much closer collisions than ionization. This is shown by the impact parameter dependence $P(b)$ in Fig. 3. Hence, capturing one electron at each center confines the orientation of the molecular axis more tightly to the beam axis than a capture followed by an ionization step at the second atom. To demonstrate this relation in a quantitative manner, we present in Figs. 2(a) and 2(b) a calculated angular distribution $F(\cos\Theta)$

$$F(\cos\Theta) = \int_0^\infty \int_0^\infty \int_{-\infty}^\infty [P_1(b_a) \cdot P_2(b_b) \cdot P(R)] dx dy dR \quad (4)$$

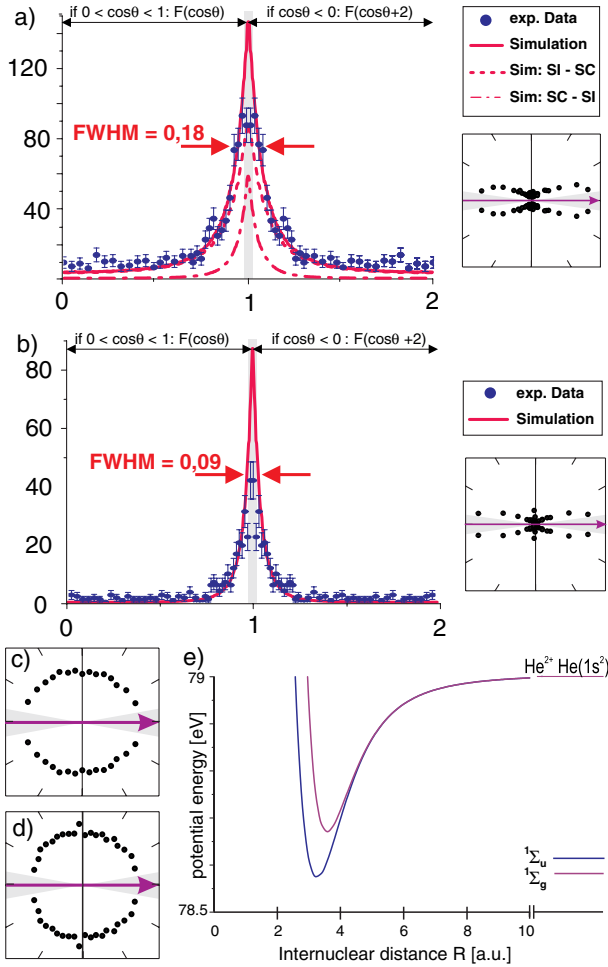


FIG. 2 (color online). Angular distribution of the fragmentation axis of the dimer with respect to the fast ion beam axis [(purple) arrow]. For $\cos\Theta < 0$, the experimental and simulated data in (a) and (b) are shifted by $(+2.0)$. (a) TI, KER = 3.5–5.0 eV. For KER < 3.5 eV the detection efficiency is heavily decreased [see Fig. 1]. In case of full efficiency the small KERs (large internuclear distances) would lead to a even more accentuated angular distribution. The simulated distribution is the sum of two curves corresponding to the different pathways. (b) DC, KER = 3.5–5.0 eV. The small peak on the right side results from background events. (c) TI, KER = 6–9 eV [peak 3 in Fig. 1]. The slight enhancement along the projectile direction originates from events of process 1 which can not be completely suppressed due to the small overlap between the KER regions. (d) KER = 9–10 eV [peak 2 in Fig. 1]. The grey area in the polar plots and in the $\cos\Theta$ distribution indicate the angular regions of decreased detection efficiency. (e) $(\text{He}^{2+}\text{He})$ potential energy curve.

with

$$b_{a,b} = \sqrt{\left(x \pm \frac{R}{2} \cos\Theta\right)^2 + y^2} \quad (5)$$

where Θ is the tilt angle between the dimer axis and the beam axis. $P_1(b_a)$ and $P_2(b_b)$ indicate the probabilities for the first and second interaction while b_a and b_b represent the

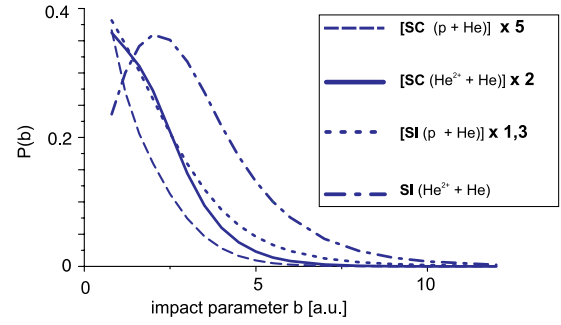


FIG. 3 (color online). Calculated impact parameter dependence $P(b)$ which were used to generate the angular distributions shown in Figs. 2(a) and 2(b). The distributions are obtained by an effective single-particle approximation [24]. To readily identify the width, the distributions were stretched. Since the $P(b)$ s for the SI and SC of $(\text{He}^+ + \text{He})$ and $(p + \text{He})$ hardly differ the $P(b)$ s of $(p + \text{He})$ were used for the calculation. For TI $F(\cos\Theta)$ was obtained by the $P(b)$ s of SC $(\text{He}^{2+} + \text{He})$, SI $(p + \text{He})$ and SI $(\text{He}^{2+} + \text{He})$, SC $(\text{He}^{2+} + \text{He})$. For DC $F(\cos\Theta)$ was calculated by the $P(b)$ s of SC $(\text{He}^{2+} + \text{He})$, SC $(p + \text{He})$.

impact parameters with respect to the atomic centers. x and y are the coordinates of the projectile while $P(R)$ is the probability for the internuclear distance R obtained from the experimental KER distribution within the reflection approximation [Eq. (3)]. The two-step TI includes a single ionization (SI) and a single capture (SC). Considering the order of these processes, two different pathways becomes possible for a two-step TI (1st SI, 2nd SC or 1st SC, 2nd SI) which corresponds to different $P(b)$ s and therefore to different $F(\cos\Theta)$. Accordingly, we obtained $F(\cos\Theta)$ for TI by adding the distributions of both pathways. The interference term has been omitted since it cannot realistically be estimated in our model. The satisfactory agreement might be taken as evidence that the interference term does not play a major role on the present level of precision. To calculate $F(\cos\Theta)$ for DC, two SC processes were assumed. The $P(b)$ distributions [Fig. 3] which were used in the calculations are obtained by an effective single-particle approximation [24] well established in the field of ion-atom collisions [25].

We now turn to the angular distributions leading to the KER peak 2 and 3 which are shown in Figs. 2(c) and 2(d). In contrast to the respective distribution of KER peak 1, they are isotropic. Following the same argumentation as before, the fragmentations here are expected to proceed via an interaction of the projectile with only one of the helium atoms. In this case the second atom of the dimer has to become charged in a subsequent step, which must be completely independent of the projectile. This conclusion is further supported by the fact that the KER for peaks 2 and 3 corresponds to $R < 5.5$ a.u. These small internuclear distances are not present in the neutral He_2 wave function [26]. This clearly shows that the charged dimer contracts before the second helium atom finally ejects an electron, triggering the Coulomb explosion.

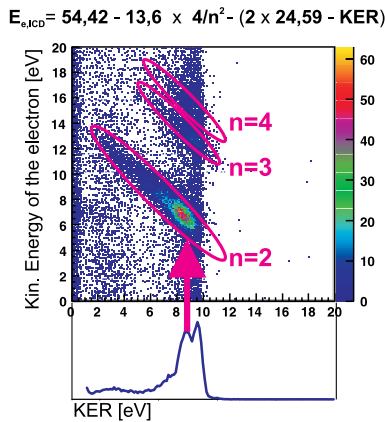


FIG. 4 (color online). Kinetic energy release (ions) versus kinetic energy of the continuum electron for TI. The diagonal feature is a characteristic of ICD (equation in the top). $n = 2, 3, 4$ indicates the ICD electrons for excitation to the intermediate state [$\text{He}^+(n)$, He].

As peak 2 is present for DC as well as for TI, the starting point must be the dimer ion consisting of a doubly charged helium ion on the one side and a neutral helium atom on the other side. Because of the polarization, the potential energy curve of this dimer ion (dissociation limit: He^{2+} , He) is attractive, even at large R where it is populated from the neutral dimer [Fig. 2(e)]. Consequently the dimer ion starts to shrink. At internuclear distances of about $R = 3.0$ a.u. (according to KER of 9.1 eV) an electron exchange between the two centers occurs [Fig. 1(c)]. The depth of the potential energy curve is about 400 meV, hence the dimer ion is expected to contract in most cases despite the momentum transfer in the collision.

KER peak 3 is present in the TI channel only. Here one electron is emitted to the continuum. Plotting the energy of this electron versus the KER [Fig. 4] shows a diagonal structure which is a typical fingerprint of the ICD [11]. As the sketch in Fig. 1(d) illustrates, the projectile captures one electron at one of the centers and simultaneously excites the remaining electron. After some contraction of the charged dimer, this locally deposited energy is transferred via virtual photon exchange to the neighboring atom leading to its ionization. Finally, the two singly charged ions trigger Coulomb explosion starting at the internuclear distance where ICD occurred. The amount of energy transferred to the neutral atom is shared by the ICD electron and the ionic fragments [see equation in Fig. 4].

In conclusion, using the cold target recoil ion momentum spectroscopy technique we measured the (He^+ , He^+) breakup of a helium dimer in fast collisions with alpha particles to explore how two-center TI and DC occurs.

The results show a second order process in which the projectile interacts with each of the dimer atoms subsequently. For dimers parallel aligned to the ion beam, this two-step process projects the He^2 ground state vibrational distribution onto the measured KER, visualizing directly its widespread delocalized nature. The angular distribution of the ionic fragments provides a novel test of theories for ion impact processes. In addition, two different processes involving an interaction of the projectile with only one atom are observed. In these cases the attractive potential between the He^{2+} and its neutral partner leads to a contraction of the dimer. The energy deposited by the ion locally at one atom is efficiently redistributed in the extended system. The most prominent of these energy redistribution mechanisms is ICD, which we find to be a major channel also for ion impact.

We thank Nikolai Kryzhevoi for providing the data for Fig. 2(e). This work was supported by the Deutsche Forschungsgemeinschaft (DFG).

*doerner@atom.unifrankfurt.de

- [1] J. C. Slater, *Phys. Rev.* **32**, 349 (1928).
- [2] P. E. Phillippon, *Phys. Rev.* **125**, 1981 (1962).
- [3] V. V. Starykh *et al.*, *J. Chem. Phys.* **72**, 2713 (1980).
- [4] A. R. Janzen *et al.*, *J. Chem. Phys.* **103**, 9626 (1995).
- [5] H. G. Bennewitz *et al.*, *Z. Phys.* **253**, 435 (1972).
- [6] F. Luo *et al.*, *J. Chem. Phys.* **98**, 3564 (1993).
- [7] W. Schöllkopf and J. P. Toennies, *Science* **266**, 1345 (1994).
- [8] R. E. Grisenti *et al.*, *Phys. Rev. Lett.* **85**, 2284 (2000).
- [9] L. S. Cederbaum, J. Zobeley, and F. Tarantelli, *Phys. Rev. Lett.* **79**, 4778 (1997).
- [10] S. Marburger *et al.*, *Phys. Rev. Lett.* **90**, 203401 (2003).
- [11] T. Jahnke *et al.*, *Phys. Rev. Lett.* **93**, 163401 (2004).
- [12] T. Jahnke *et al.*, *Nature Phys.* **6**, 139 (2010).
- [13] M. Mücke *et al.*, *Nature Phys.* **6**, 143 (2010).
- [14] T. D. Märk *et al.*, *Nature Phys.* **6**, 82 (2010).
- [15] B. Boudaiffa *et al.*, *Science* **287**, 1658 (2000).
- [16] R. Dörner *et al.*, *Phys. Rep.* **330**, 95 (2000).
- [17] J. Ullrich *et al.*, *Rep. Prog. Phys.* **66**, 1463 (2003).
- [18] O. Jagutzki *et al.*, *IEEE Trans. Nucl. Sci.* **49**, 2477 (2002).
- [19] N. Sisourat *et al.*, *Nature Phys.* **6**, 508 (2010).
- [20] T. Havermeier *et al.*, *Phys. Rev. Lett.* **104**, 133401 (2010).
- [21] S. Martinez *et al.*, *Phys. Rev. A* **72**, 062722 (2005).
- [22] J. Caillat *et al.*, *Phys. Rev. A* **73**, 014701 (2006).
- [23] S. Cheng *et al.*, *Phys. Rev. A* **47**, 3923 (1993).
- [24] H. J. Lüdde, *Springer Series on Atomic, Optical, and Plasma Physics* **35**, 205 (2003).
- [25] T. Kirchner *et al.*, *Recent Res. Devel. Physics* **5**, 433 (2004).
- [26] F. Luo *et al.*, *J. Chem. Phys.* **98**, 9687 (1993).